Disorder induced interface states and their influence on the Al/Ge nanowires Schottky devices

R. A. Simon, H. Kamimura, O. M. Berengue, E. R. Leite, and A. J. Chiquito

Citation: Journal of Applied Physics **114**, 243705 (2013); doi: 10.1063/1.4857035
View online: http://dx.doi.org/10.1063/1.4857035
View Table of Contents: http://scitation.aip.org/content/aip/journal/jap/114/24?ver=pdfcov
Published by the AIP Publishing

Disorder induced interface states and their influence on the Al/Ge nanowires Schottky devices

R. A. Simon,[1] H. Kamimura,[1] O. M. Berengue,[2] E. R. Leite,[3] and A. J. Chiquito[1]
[1]*NanO LaB - Departamento de Física, Universidade Federal de São Carlos, CEP 13565-905, CP 676 São Carlos, São Paulo, Brazil*
[2]*Departamento de Física e Química, Faculdade de Engenharia de Guaratinguetá, Universidade Estadual Paulista Júlio de Mesquita Filho, CEP 12516-410 Guaratingueta, São Paulo, Brazil*
[3]*Laboratório Interdisciplinar de Eletroquímica e Cerâmicas, Departamento de Química, Universidade Federal de São Carlos, CEP 135665-905, CP 676 São Carlos, São Paulo, Brazil*

(Received 18 August 2013; accepted 9 December 2013; published online 26 December 2013)

It has been demonstrated that the presence of oxide monolayers in semiconductor surfaces alters the electronic potential at surfaces and, consequently, can drastically affect the electronic transport features of a practical device such as a field effect transistor. In this work experimental and theoretical approaches to characterize Al/germanium nanowire Schottky devices by using samples covered with a thin oxide layer (2 nm width) were explored. It was also demonstrated that the oxide layer on Ge causes a weak dependence of the metal work function on Schottky barrier heights indicating the presence of Fermi level pinning. From theoretical calculations the pinning factor S was estimated to range between 0.52 and 0.89, indicating a weak Fermi level pinning which is induced by the presence of charge localization at all nanowires' surface coming from interface states. © *2013 AIP Publishing LLC*. [http://dx.doi.org/10.1063/1.4857035]

I. INTRODUCTION

Nanowires and nanobelts-based devices are at the center of the new developments in the nanoscale research. Low dimensional systems are ideal platforms to obtain an interface (building blocks) between the molecular world and useful solid state devices. Germanium nanostructures can be very interesting from a technological point of view mainly because of their interesting characteristics such as small and indirect band gap (0.67 eV), high electron mobility in comparison to silicon, and large characteristic Bohr radius (24.3 nm) also compared with Si (4.9 nm). This last feature causes quantum size effects to be more prominent in Ge nanowires.[1–9] However, fabrication of reliable electrical contacts to nanowires remains a challenging task mainly due to the presence of some degree of surface disorder which affects the carriers transport in nanowires, making difficult the control of the Fermi level of the whole system. The presence of surface disorder in such nanostructures is commonly addressed to surface native oxides which unintentionally grow on the nanowires surface and sometimes drastically affect the injection of current trough the nanostructure.[10] It is worth to remember that the high surface to volume ratio in nanostructures enhance surface effects and the influence of all surfaces in the transport mechanism should be equally considered. Usually, the disorder leads to a localized behaviour of carriers transport, and a transition from a simple excitation semiconducting mechanism to a more complex one such as the variable range hopping mechanism (VRH) can be observed. This mechanism arises when there is a sufficient amount of disorder states causing the random component of the crystalline potential to be large enough to localize the electrons wave functions near the band edges.[11–14] In fact, we recently show that not only the contribution of the localization of charges on a nanostructures surface alter its conduction process[15–17] but also the VRH mechanism can be observed in as-grown Ge nanowires as a consequence of this behaviour.[12] In this work electron transport measurements and numerical calculations were associated in order to study the effects of the interface states on the characteristics of the electrical contacts fabricated to Ge nanowires covered with a thin oxide layer (<2 nm). The calculations showed that the contribution of surface states has to be taken in all surfaces, leading to a non negligible band bending near the nanowire's surface which, in turn, results in an effective Schottky barrier height. In a general way, these findings can also be extended to the interpretation of the sensing mechanism (involving exchange of charges through the nanowire's surface with different environments, for instance) usually observed in these structures.[18–20] Experimental data on electronic transport in Ge nanowires were also analysed using our theoretical approach, providing the opportunity to establish a quantitative understanding of the influence of surface states on nanowire electrical properties.

II. EXPERIMENT

Ge nanostructures were fabricated by using the vapour-liquid-solid (VLS) approach, first demonstrated by Wagner and Ellis.[21] The growth apparatus used for this experiment consisted of a single-zone tube furnace (Lindberg/Blue M) through which a controlled flow of Ar drives the precursor materials to the hot zone (950 °C). A quartz tube containing both the SiO_2 (100) substrates (with catalyst nanoparticles formed by thermal annealing of an evaporated 20 Å thick gold layer) and the germanium powder was used to hold the samples and to confine the produced vapour. In order to decrease the non intentional native oxide layer on Ge nanowire's surface the tube was continuously pumped (10^{-2} Torr) and purged (50 sccm Argon gas flux (purity >99.998%) at a fixed temperature (200 °C). After a growth of 40 min at

950 °C, Ge nanowires were grown on the substrate. The morphology of the products was investigated by Field Emission Gun Scanning Electron Microscopy (FEG-SEM, Zeiss Supra 35, equipped with an energy-dispersive X-ray spectrometer (EDS)). The micrography of the as-prepared Ge nanowires on SiO_2 substrates is depicted in Figs. 1(a) and 1(c). As observed in Fig. 1(a) the diameter of as-grown nanowires was found to range between 50 and 200 nm, and the length is of tens of micrometers. Figure 1(c) depicts the EDS analysis of the samples where a negligible content of oxide species was found. The structure of the as-synthesized Ge nanowires was examined using X-ray diffraction (XRD, Rigaku diffractometer model DMAX 2500PC, 40 kV, 150 mA, with a Cu Kα radiation) and transmission electron microscopy (TEM, Tecnai F20G2, Phillips). The XRD pattern shown in Fig. 1(b) indicates that the samples are single crystalline in the diamond-like cubic phase[22] with the lattice constant $a = 0.565$ nm (Fd-m space group). The TEM measurements also confirmed the samples high crystalline quality. The inset in Fig. 1(d) displays a TEM image of an individual Ge nanowire (inset) from which it was found that the nanowires grow along the [110] orientation. Also, the presence of a thin non-intentionally grown oxide layer (GeO_x) was found. This layer is known to be always present in germanium:[23] in our case the TEM analysis shows a disordered oxide layer, thickness of less than 2 nm, in agreement with the previous data from XRD and EDS. In order to perform temperature-dependent transport measurements aluminium contacts were fabricated directly on the as-grown samples. Considering the potential integration of Ge nanowires with present Si technology, aluminium was chosen for the contacts because it is one of the most used metals for electronic devices fabrication. Different geometries for the contacts were patterned (interdigital or dots electrodes) on samples, but in both geometries the results remain unchanged. The temperature-dependent transport measurements were carried out in a closed cycle helium cryostat (Janis Research, CCS 400H) working at a pressure lower than 10^{-6} Torr. The resistance curves were monitored by an electrometer (Keithley Instruments, 6517B) using the four contacts geometry. For current-voltage characterization two contacts geometry was used.

III. RESULTS AND DISCUSSION

As stated by many authors,[24,25] the oxide layer presents in Ge nanostructures can be reduced with chemical reactions or thermal annealing but not completely avoided: after a short period of time the oxide layer re-grow. From a practical point of view it is very interesting to study the real case in which a thin oxide layer is present. Also, further advances of existing technologies call for the capacity to control both assembly and integration of structures on scales reaching more than individual nanowire devices. As an example, a device made from several nanowires is suitable for practical applications such as sensors since it has a better signal-to-noise ratio, a larger activation area, and a longer lifetime, being easier not only to manipulate but also to integrate with other devices.[26–28] In this sense a four-terminal device was fabricated in which the active elements are the oxide-capped germanium nanowires. Figure 2 depicts data on temperature-dependent transport measurements and a sketch of the Ge-based device.

To estimate the resistivity, the well-known equation $\rho = RA/L$ was applied considering several single devices ($L = 5\,\mu$m and cross section areas from 10^{-14} to 10^{-15} m^2) using resistance data. The values of $\rho(300\,K)$ were found from 2×10^4 to $7 \times 10^4\ \Omega$ cm. For the carrier density evaluation the equation $n = 1/\rho e\mu$ was used considering the carrier mobility to be 0.01 cm^2/V s (Ref. 12) and the above resistivity values, resulting in 1–3 $\times 10^{16}$ cm^{-3}. Fig. 2(a) reveals the semiconducting character of the samples. The experimental

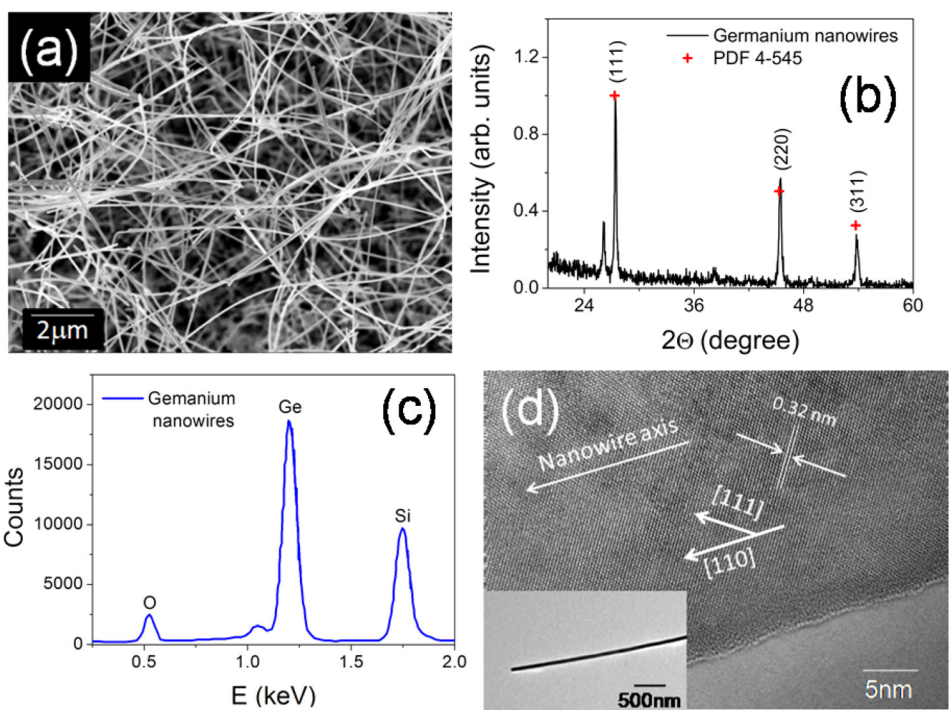

FIG. 1. (a) SEM image of as grown Ge nanowires showing diameters between 80 and 240 nm and lengths of tens of micrometers. (b) XRD pattern of Ge nanowires samples, agreeing with PDF 4-545 where the cubic structure of germanium is observed (the small peak at ~26° represents the contribution of GeO_2 oxide). (c) EDS spectrum on nanowires is showed in (a) confirming the negligible GeO_x oxide quantity. (d) HRTEM image of a single nanowire showing a thin oxide layer (<2 nm) and the important crystallographic planes. The lattice spacing was found to be 0.32 nm, corresponding to the (111) plane family. Lattice fringes formed an angle of 54° with the nanowire's growth axis so that the growth direction of the nanowire was found to be along [110]. In the inset, a low resolution image of the nanowire is depicted.

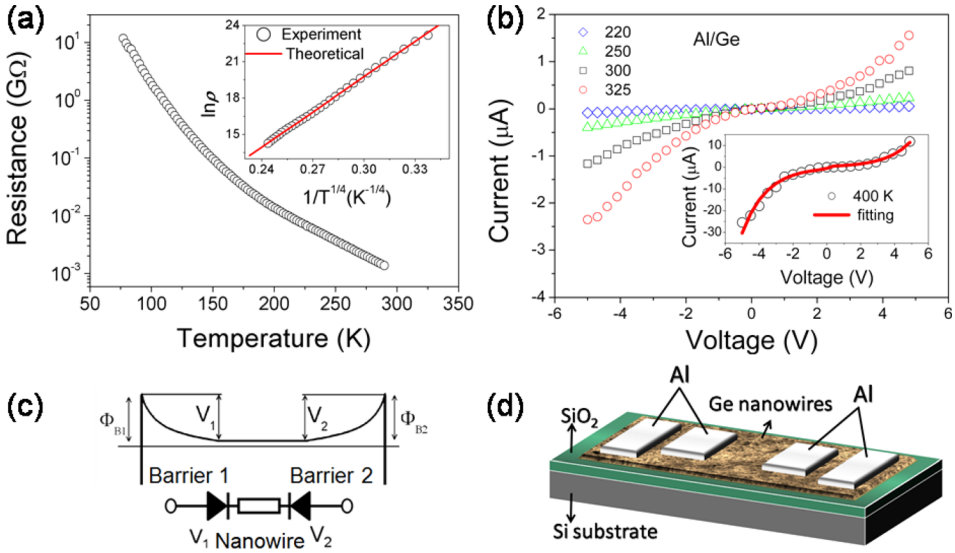

FIG. 2. (a) Temperature-dependent resistance curve revealing a semiconductor behaviour and the corresponding fitting for the VRH mechanism (inset). (b) Current-voltage curves for different temperatures used to determine the Schottky barrier height, using the back-to-back model. The fitting for 400 K is shown in the inset. (c) The equivalent electrical circuit for the back-to-back model. (d) Sketch of the experimental device with aluminium contacts over Ge nanowires layer on Si/SiO_2 substrate.

curve does not follow the expected simple thermal excitation law for a semiconductor. The observed behaviour was well fitted to the VRH conduction mechanism due to Mott.[11] In this model, phonons are required to conserve energy during a hop from site to site: the higher phonon density at a higher temperature increases the hopping rate and thereby decreases the resistivity. The VRH mechanism is described by[11]

$$\rho(T) = \rho_0 \exp\left(\frac{T_0}{T}\right)^{1/4}, \tag{1}$$

where $T_0 = \frac{5.7\alpha^3}{k_B N(E_F)}$, $N(E_F)$ is the density of states at the Fermi level, k_B is the Boltzmann constant, and α^{-1} the localization length. The conduction takes place by hopping of small region (k_BT) in the vicinity of the Fermi level where the density of states remains almost a constant. This condition is fulfilled when the temperature is sufficiently small or when the energy states are uniformly distributed. The agreement between theoretical and experimental curves [inset of Fig. 2(a)] confirms that the VRH process governs the transport in whole range of temperatures (77–300 K), providing us with a hopping length ~60 nm (at 300 K).[11] This length is the mean distance that electrons must hop in order to contribute to the conductivity.[11] Also it is in reasonable agreement with the Bohr radius of germanium (24 nm), and it is smaller than the nanowires. The large value of the localization length could be a manifestation of a change in the nature or in the type of localization centers through which the conduction occurs.[29]

As revealed by the TEM analysis, the surface of germanium nanowires is naturally covered by a thin oxide layer produced during the synthesis process but also due to the contact to the atmosphere. As above mentioned, the Ge/GeO_x interface is disordered due to its nature, and it induces a disordered potential that should affect the conduction of electrons inside the Ge nanowires.[15] In fact, a small surface disorder could dominate nanowire bulk properties as the sizes of the samples are scaled down (by controlling the Fermi level and screening out electrons from surface, for instance). As an example of this problem, it is interesting to mention that current-voltage curves obtained in devices produced under the same conditions and using identical metallic contacts can be very different presenting electrical characteristics ranging from Schottky to ohmic behaviour.[30] This implies that metal/semiconductor contacts depend in large part on interfacial chemistry.[31,32] It should be noted that the natural surface disorder can trap charges "spreading" the interface states into a few nanometers inside the semiconductor. In this scenario the current-voltage dependence is useful for extraction of electrical parameters of these devices, and they can be seen in Fig. 2(b) for different temperatures. Clearly, two Schottky barriers were observed. This metal/semiconductor/metal can be modelled using the back-to-back Schottky model under the usual thermionic emission theory assumptions. The total current is[34]

$$J(V,T) = \frac{2J_{01}J_{02}\sinh\left(\frac{qV}{2k_BT}\right)}{J_{01}\exp\left(\frac{qV}{2k_BT}\right) + J_{02}\exp\left(\frac{-qV}{2k_BT}\right)}, \tag{2}$$

where

$$J_{01,02}(V) = A^*T^2\exp\left(\frac{-q\Phi_{B1,B2}}{k_BT}\right). \tag{3}$$

According to Rhoderick,[35] image-force effects always result in a voltage dependence of the barrier height which is then an effective barrier as follows:

$$\Phi_{B1,B2} = \Phi_{B10,B20} + V_{1,2}\left(\frac{1}{n_{1,2}} - 1\right). \tag{4}$$

In this equation, $n_{1,2}$ are the ideality factors, Φ_{B01} and Φ_{B02} are the values of barriers in an ideal Schottky junction, and $V_{1,2}$ are the voltage drops at the junctions. Fitting the current-voltage curves in Fig. 2(b) using Eq. (2) Φ_{B01} between 0.54 eV (220 K) and 0.48 eV (400 K) was found and Φ_{B02} between 0.55 eV (220 K) and 0.51 eV (400 K).

In order to interpret the experimental data on barrier heights a model based on a distribution of charges near the

surface of the nanowires was developed, accounting for the disorder induced interface states.[33] Lu and Barret[32] used a similar idea in order to study the consequences of a distribution of interface states in metal/GaAs Schottky barriers.[32] In that work, the interface states were spread out in thin few layers inside the semiconductor under the metallic contact. Taking into account the size of Ge nanowires, the objective here was to determine some parameters (such as the Schottky barrier) by considering the non-uniformities on the charges distribution in all nanowires surfaces. For this purpose the Poisson equation was solved by considering a single germanium nanowire device with two electrical contacts as sketched in the inset of Fig. 3(a). The Schottky contact was characterized by a barrier height of 0.58 eV (Ref. 36), and a rectangular shaped intrinsic germanium nanowire surrounded by vacuum was used. For this geometry, the Poisson equation is written as

$$\nabla.[\epsilon(\vec{r})\nabla\Phi(\vec{r})] = \rho(\vec{r}), \tag{5}$$

where $\epsilon(\vec{r})$ is the electrical permissibility, $\Phi(\vec{r})$ is the electrical potential, and $\rho(\vec{r})$ is the electrical charge density. This density should include the contribution of electrons in the conduction band and additional effects of charges trapped in interface states. In order to account effects of surface charges an energy and space distribution for interface states were considered as follows:

$$\rho_{SS}(\vec{r}) = q\frac{N_{SS}}{L_D}\int\int_S d\vec{r'}\exp\left(\frac{-d(\vec{r},\vec{r'})}{L_D}\right) \times \left[1+\exp\left(\frac{E_f-(\Phi(\vec{r})-E_D)}{kT}\right)\right]^{-1}, \tag{6}$$

where N_{SS}/L_D is the surface density/penetration depth of an interface state, $d(\vec{r},\vec{r'})$ is the distance between the points $\vec{r}$ and $\vec{r'}$, and $\int\int_S d\vec{r'}$ represents the integral over the nanowire surface, E_D is the activation energy of a given state, and E_f is the Fermi level.

The distribution presented in Eq. (6) was used in *all* the surfaces defining the nanowire: in this one-dimensional geometry, the effect of trapped charges in the lateral oxide/nanowire interfaces as above mentioned (usually the surface states are considered only at the metal/semiconductor interface) cannot be neglected. Even in the case where no oxide layer was detected, the interface air/nanowire interactions, leading to charge localization, should be considered. In fact, all applications of nanowires as sensing elements invariably depend on the ability of the electron transport in nanowire to be modified by effects of such surface charges.

Equation (5) was numerically solved assuming different values for the density of interface states (from 10^{12} to 10^{14} states/cm^2) and penetration depth L_D (1 nm, 5 nm, 10 nm). Also, different values for E_D were used. For these calculations the dimensions of the nanowires were x = 500 nm, y = 50 nm, and z = 5 μm. The numerical solution was obtained within the finite difference framework, as follows: the nanowires and their surroundings were divided into a mesh of discrete points, and for each point in the mesh, the values of potential were calculated. At interfaces, the following boundary conditions were applied: *z direction*—at the face corresponding to the Schottky contact, $\Phi = \Phi_B = 0.58$ eV (barrier height); at the ohmic contact, $\nabla\Phi = 0$ what means flat band; *x-y plane*—in this plane, the same condition is applied but considering a distance of 1 μm far from nanowire in both directions, where a vanishing electric field was assumed. The non linear equation system was

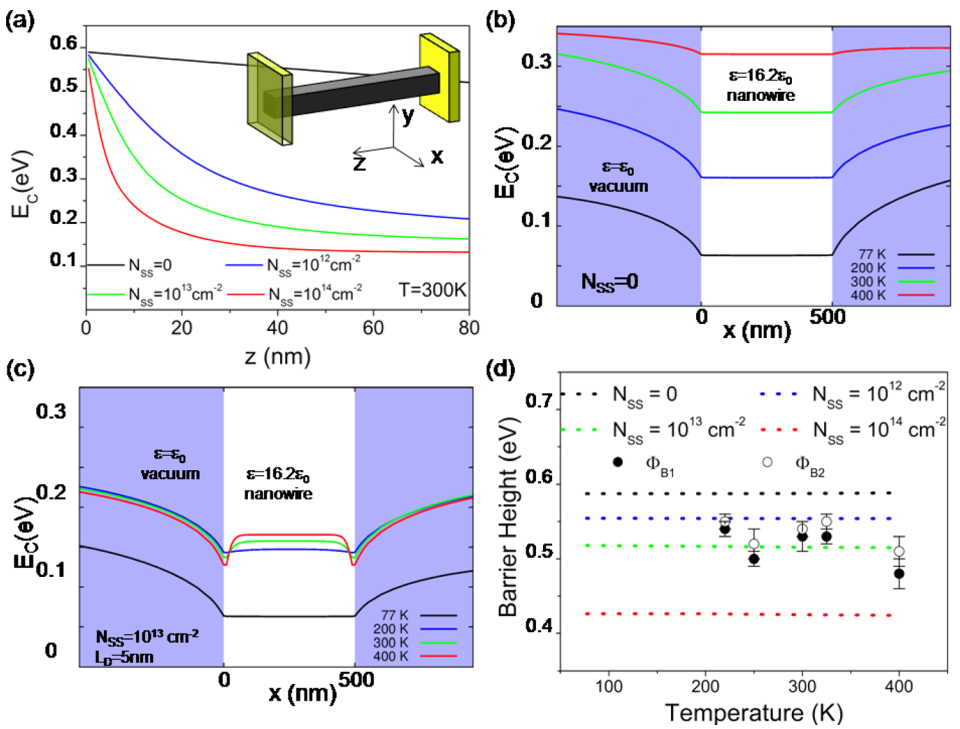

FIG. 3. In panels (a) and (b) are shown the conduction band energy profile in x-y plane far from the depletion region produced by the Schottky contact at z = 0 (out of the page) and at 300 K. The effects of the interface states are readily observed in the nearby surface region. (c) The conduction band energy profile in the x direction for different interface states density also at 300 K. The energy around z = 0 is the effective Schottky barrier. (d) Comparison between the theoretical and experimental Schottky barriers for different temperatures and interface states densities.

solved by using the Newton-Raphson method,[37] using as stopping criterion a convergence of 0.05% between two consecutive steps. The main results are summarized in Fig. 3.

Cross section plots (x-y planes) for the nanowire conduction band in the neutral region (far from the depletion region due to the Schottky barrier) for different temperatures are seen in Fig. 3(b) ($N_{SS}=0$) and Fig. 3(c) ($N_{SS}\neq 0$). The displayed results were obtained for $L_D=5$ nm, $E_D=0.3$ eV which provided the better adjustment to the experimental values. The effects of the interface states can be readily observed by the strong changes in the conduction band profile at the surface of the nanowires.

The energy at the vacuum/nanowire interface can be considered an estimate for the surface potential (Φ_S), and it reflects the presence of charges randomly distributed by the interface states. This behaviour was expected: interface states and the corresponding dipole charges were distributed in nearby surface layers inside the semiconductor, thus creating a charged and disordered electrical shell (few nanometers thick) around nanowires.[38,39]

Fig. 3(c) shows the conduction band profile in z direction for different interface states densities at 300 K. The analysis of these results should be carefully accounted because $\Phi(z=0)$ values do not represent correctly the Schottky barrier height. The space between interface ($z=0$) and $z=L_D$ is a thin layer where interface states are acting as specified in our model, and in fact, it is essentially transparent for carriers. Then, the Schottky barriers were calculated within $0<z<L_D$ taken from the semiconductor surface and Φ_B values found should be considered as effective barrier heights.[32] Theoretical and experimentally obtained Schottky barriers are plotted in Fig. 3(d) at different temperatures, interface states densities and for $z=2.0$ nm (in $0<z<L_D$ range there is no significant change on their values). From Fig. 3(d) then the density of interface states can be estimated of our samples between 10^{12} and 10^{13} states/cm^2. Such a density leads to pinning factors between $S=0.89$ and $S=0.52$ by considering that the density of interface states N_{SS} in the band gap of a semiconductor can roughly be estimated from the well known relationship[40]

$$N_{SS}=1.1\times 10^{13}\left(\frac{1-S}{S}\right)\mathrm{cm}^{-2}. \quad (7)$$

These S values show a weak Fermi level pinning (the strong pinning is obtained when the Bardeen limit, $S=0$, is reached[31]) in opposition to results found in metal/bulk Ge.[41,42] We believe that in bulk samples only the metal/-semiconductor interface charges contributes to the barrier formation. Our calculations showed that the random distribution of charges in the surfaces of the nanowires contributes to the barrier formation: due to the size of the samples, disorder in any surface induces a perturbation which propagates to the whole system affecting even the space charge region below the metal contact. Then, the net charge located at electronic levels which were introduced into the gap due to the surface disorder determines the overall electronic behaviour of the metal/Ge nanowires.

IV. CONCLUSION

The effects of interface states on Schottky contacts fabricated to high quality germanium nanowires were studied. The presence of unavoidable disorder (coming from a non-intentional grown thin oxide layer) at the nanowire's surfaces was pointed as the responsible for localizing charges at the interface, leading to the Fermi level pinning. As observed in this work, the presence of interface states affects directly the formation of the Schottky barrier, but their presence influences the overall electron transport in the nanowires as confirmed by the observed hopping mechanism. Using an electrostatic model for the charges distribution on the surfaces of the nanowires, the experimental values of Schottky barrier were theoretically confirmed.

ACKNOWLEDGMENTS

The authors thank R. H. Gonçalves and B. R. H. Lima for TEM and FEG-SEM images and the Brazilian research funding agencies (Grant 2009/51740-9, São Paulo Research Foundation (FAPESP)) and CNPq (302640/2010-0) for the financial support of this work.

[1]Y. Wu and P. Yang, Chem. Mater. **12**, 605 (2000).
[2]L. J. Lauhon, M. S. Gudiksen, C. L. Wang, and C. M. Lieber, Nature **420**, 57 (2002).
[3]A. B. Greytak, L. J. Lauhon, M. S. Gudiksen, and C. M. Lieber, Appl. Phys. Lett. **84**, 4176–4178 (2004).
[4]W. Lu, J. Xiang, B. P. Timko, Y. Wu, and C. M. Lieber, Proc. Natl. Acad. Sci. U.S.A. **102**, 10046 (2005).
[5]O. Hayden, A. B. Greytak, and D. C. Bell, Adv. Mater. **17**, 701 (2005).
[6]E. Tutuc, J. Appenzeller, M. C. Reuter, and S. Guha, Nano Lett. **6**, 2070 (2006).
[7]J. Xiang, W. Lu, Y. J. Hu, Y. Wu, H. Yan, and C. M. Lieber, Nature **441**, 489 (2006).
[8]Y. J. Hu, H. O. H. Churchill, D. J. Reilly, J. Xiang, C. M. Lieber, and C. M. Marcus, Nat. Nanotechnol. **2**, 622 (2007).
[9]H. Yan, H. S. Choe, S. W. Nam, Y. Hu, S. Das, J. F. Klemic, J. C. Ellenbogen, and C. M. Lieber, Nature **470**, 240–244 (2011).
[10]G. Gu, M. Burghard, G. T. Kim, G. S. Dusberg, P. W. Chiu, V. Krstic, and S. Roth, J. Appl. Phys. **90**, 5747 (2001).
[11]N. F. Mott, *Metal-Insulator Transitions*, 2nd ed. (Taylor and Francis, London, 1990).
[12]H. Kamimura, L. S. Araujo, O. M. Berengue, C. A. Amorim, A. J. Chiquito, and E. R. Leite, Physica E (Amsterdam) **44**, 1776 (2012).
[13]A. J. C. Lanfredi, R. R. Geraldes, O. M. Berengue, E. R. Leite, and A. J. Chiquito, J. Appl. Phys. **105**, 023708 (2009).
[14]A. D. Schricker, S. V. Joshi, T. Hanrath, S. K. Banerjee, and B. A. Korgel, J. Phys. Chem. B **110**, 6816 (2006).
[15]O. M. Berengue, R. A. Simon, E. R. Leite, and A. J. Chiquito, J. Phys. D **44**, 215405 (2011).
[16]Y. A. Pusep, A. J. Chiquito, S. Mergulhao, and J. C. Galzerani, Phys. Rev. B **56**, 3892 (1997).
[17]Y. A. Pusep, A. J. Chiquito, S. Mergulhao, and A. I. Toropov, J. Appl. Phys. **92**, 3830 (2002).
[18]F. Hernandez-Ramirez, J. D. Prades, R. Jimenez-Diaz, T. Fischer, A. Romano-Rodriguez, S. Mathur, and J. R. Morante, Phys. Chem. Chem. Phys. **11**, 7105 (2009).
[19]A. Kolmakov, D. O. Klenov, Y. Lilach, S. Stemmer, and M. Moskovits, Nano Lett. **5**, 667 (2005).
[20]A. Vomiero, S. Bianchi, E. Comini, G. Faglia, M. Ferroni, N. Poli, and G. Sberveglieri, Thin Solid Films **515**, 8356 (2007).
[21]R. S. Wagner and W. C. Ellis, Appl. Phys. Lett. **4**, 89 (1964).
[22]Joint Committee on Powder Diraction Standards (JCPDS), Card No. 4–545.
[23]D. Wang, Y. Chang, Q. Wang, J. Cao, D. B. Farmer, R. G. Gordon, and H. Dai, J. Am. Chem. Soc. **126**(37), 11602–11611 (2004).

[24]T. Hanrath and B. A. Korgel, J. Am. Chem. Soc. **126**, 15466 (2004).
[25]D. Wang, Q. Wang, A. Javey, R. Tu, H. Dai, H. Kim, P. C. McIntyre, T. Krishnamohan, and K. C. Saraswat, Appl. Phys. Lett. **83**, 2432 (2003).
[26]N. V. Hieu, L. T. N. Loan, N. D. Khoang, N. T. Minh, D. T. Viet, D. C. Minh, T. Trung, and N. D. Chien, Curr. Appl. Phys. **10**, 636 (2010).
[27]D. Zhang, Z. Liu, C. Li, T. Tang, X. Liu, S. Han, B. Lei, and C. Zhou, Nano Lett. **4**, 1919 (2004).
[28]D. Whang, S. Jin, Y. Wu, and C. M. Lieber, Nano Lett. **3**, 1255 (2003).
[29]B. Yu, X. H. Sun, G. A. Calebotta, G. R. Dholakia, and M. Meyyappan, J. Cluster Sci. **17**, 579 (2006).
[30]Z. Zhang, K. Yao, Y. Liu, C. Jin, X. Liang, Q. Chen, and L.-M. Peng, Adv. Funct. Mater. **17**, 2478 (2007).
[31]J. Bardeen, Phys. Rev. **71**, 717 (1947).
[32]G. N. Lu, C. Barret, and T. Neffati, Solid-State Electron. **33**, 1 (1990).
[33]H. Hasegawa and H. Ohno, J. Vac. Sci. Technol. B **4**, 1130 (1986).
[34]A. J. Chiquito, C. A. Amorim, O. M. Berengue, L. S. Araujo, E. P. Bernardo, and E. R. Leite, J. Phys.: Condens. Matter **24**, 225303 (2012).
[35]E. H. Rhoderick and R. Williams, *Metal-Semiconductor Contacts*, 2nd ed. (Pergamon Press, Oxford, 1988).
[36]T. Nishimura, K. Kita, and A. Toriumi, Appl. Phys. Lett. **91**, 123123 (2007).
[37]R. L. Burden and J. D. Faires, *Numerical Analysis*, 9th ed. (Cengage Learning, Canada, 2011).
[38]T. Sato, S. Kasai, and H. Hasegawa, Appl. Surf. Sci. **175/176**, 181 (2001).
[39]T. Sato, S. Kasai, H. Okada, and H. Hasegawa, Jpn. J. Appl. Phys., Part 1 **39**, 4609 (2000).
[40]A. M. Cowley and S. M. Sze, J. Appl. Phys. **36**, 3212 (1965).
[41]A. Dimoulas, P. Tsipas, A. Sotiropoulos, and E. K. Evangelou, Appl. Phys. Lett. **89**, 252110 (2006).
[42]E. D. Marshall, C. S. Wu, C. S. Pai, D. M. Scott, and S. S. Lau, Mater. Res. Soc. Symp. Proc. **47**, 161 (1985).